Journal of Magnetism and Magnetic Materials 475 (2019) 93–97

Contents lists available at ScienceDirect

Journal of Magnetism and Magnetic Materials

journal homepage: www.elsevier.com/locate/jmmm

Research articles

Wetchemical synthesis of FePt nanoparticles: Tuning of magnetic properties and biofunctionalization for hyperthermia therapy

Madhuri Mandal Goswami[a,*], Arpita Das[b], Debarati De[b]

[a] S. N. Bose National Centre for Basic Sciences, Sector-III, Block – JD, Salt Lake, Kolkata 700106, India
[b] CRNN, University of Calcutta, Sector-III, Block – JD, Salt Lake, Kolkata 700106, India

ARTICLE INFO

Keywords:
Micelles
FePt
Nanoparticles
Fct phase
Hyperthermia therapy

ABSTRACT

This work reports a new approach of synthesis of FePt nanoparticles in aqueous medium using cetyl trimethylammonium bromide (CTAB) surfactant as a capping agent and the influence of change of its concentration on the size of the particles. Tuning of magnetic properties has also been done by changing the CTAB concentrations. Here at higher CTAB concentration, particles formed are of smaller size compared to the size prepared in lower micellar concentration. The ordering parameter of the particles after annealing at 550 °C with the variation of particle size is also studied. The magnetic properties of these particles are studied and the effect of particle phase and size on magnetic property is also investigated. The particles are prepared in aqueous medium because water soluble particles are useful for hyperthermia therapy. Heating abilities of the particles under AC magnetic field are also checked with change in their size. The studies on interaction of particles with cancer cell line was also performed with probing the cell by fluorescence imaging technique after bio-functionalization of the particles by sodium oleate and fluorescent dye rhodamine-B-isothiocyanate (RITC). All these preliminary studies indicate a promising applicability of the particles for localized cancer treatment by magnetic field induced hyperthermia therapy.

1. Introduction

The application of magnetic nanoparticles (MNPs) in biological field of research is of growing importance [1]. MNPs have several promising applications [2], such as magnetic separation [3], sensing [4], hyperthermia, [5], magnetic resonance imaging (MRI) [6] and many others because magnetic property play a crucial role for their selective application. Therefore tuning of magnetic properties is very important for the application of magnetic nanoparticles in different biological fields. Different magnetic nanoparticles especially iron oxide types are being investigated to explore their applicability in many theranostic purposes through imaging techniques and drug-delivery. But their poor magnetic properties at very small size limit their applications sometimes. On the other hand, scientists are mostly concentrating on soft magnetic materials for using them in biological fields. There are also many hard magnetic materials like FePt, CoPt, NiPt, Co, Fe etc. People are interested for the synthesis of such hard materials mainly because of their use in high density storage media, permanent magnet, spintronic devices etc. We are trying to explore suitability of hard magnetic materials for hyperthermia therapy. We think that these groups of hard magnetic materials will dissipate the heat with higher rate compared to soft magnetic materials because of higher hysteresis loss in case of hard magnetic material. The higher heating rate of materials will help to kill the cancer cells in higher rate and that is actually required to control the growth rate of cancer cells. But for biological application of such materials, it must be biocompatible and water soluble. Proper functionalization of the materials will provide the biocompatibility. Recently, Xu et al. reported the use of nitrilotriacetic acid-functionalized FePt nanoparticles as a general agent to separate polyhistidinelabeled proteins.[4a] Farle and co-workers reported the use of tetramethylammonium hydroxide to stabilize FePt nanoparticles in aqueous solutions. However, the aqueous stability of these nanoparticles, including that in biological media, has not been established well. Furthermore, a general route to decorate FePt nanoparticles with diverse functionalities has yet to be explored. Recent advancements in synthesis of nanomaterials have brought about a significant impact for potential clinical applications in both diagnostics and therapeutics [7–12]. For synthesis of FePt particles, people so far use solution phase based high temperature decomposition of $Fe(CO)_5$ and reduction of Pt(acac)2 [13,14] and this has been demonstrated as a general approach for synthesis of other alloyed nanoparticles as CoFe, CoPt FeMo, CoFePt, AgFePt, etc. However, $Fe(CO)_5$ is volatile and thermally unstable. It

* Corresponding author.
E-mail address: madhuri@bose.res.in (M.M. Goswami).

https://doi.org/10.1016/j.jmmm.2018.11.024
Received 23 June 2018; Received in revised form 16 October 2018; Accepted 4 November 2018
Available online 05 November 2018
0304-8853/

decomposes to CO and Fe at high temperature and CO and $Fe(CO)_5$ is a well known toxic reagent for environment. More over the high temperature synthesis needs excess $Fe(CO)_5$ to establish desired final composition of Fe and Pt in FePt particles. It is therefore desired to synthesize material using less toxic metal precursors and the initial molar ratio of metal precursor to be carried over to the final product. In the present study we have used $Fe(acetate)_2$ as Fe source $Pt(acac)_2$ as Pt source and sodium borohydride as reducing agent which can maintain well the composition of Fe:Pt in final product from the corresponding precursor salts in expected composition.

We have shown in our previous studies that synthesis of nanoparticles using the restricted environment offered by micellar systems offers excellent control over particle size [15–17]. We have used in this report reverse micellar system of cetyltrimethylammonium bromide (CTAB) surfactant in varying amounts, diphenyl eher, ethyl alcohol and water to synthesize FePt alloyed nanoparticles of various sizes. Pileni and their coworker have employed micelles or dendrimer as template to control the size and shape of particles [18]. We have utilized here water soluble micelles CTAB for preparing FePt nanoparticles of variable sizes to explore a new synthesis route for preparation of water soluble particles. We have shown here change of magnetic properties for the particles with change of their size, structure, phase and heat dissipation properties with change of magnetic properties.

2. Experimental

2.1. Reagent

$Fe(acetate)_2$, $Pt(acac)_2$, CTAB, diphenyl ether, alcohol histopaque-1077 and rodamin B- isothiocyanate (RITC) were purchased from [Sigma Aldrich]. Phosphate buffer solution (PBS), dimethyl sulfoxide (DMSO), ethanols [Merck, Germany], culture media Dulbecco's Modified Eagle's Medium (DMEM), non essential amino acids, Amphotericin B, RPMI-1640, penicillin, streptomycin, gentamycin, L-glutamine [HIMEDIA (Mumbai, India)] and Fetal bovine serum (FBS) [Invitrogen (Carlsbad, CA, USA)] were purchased.

2.2. Instrument

The XRD analysis was performed in Rigaku Miniflex II desktop X-ray diffractometer using Cu K_α ($\lambda = 1.5418$ Å) source. The TEM investigations of the particles were done by TECHNAI G^2 SF20 ST TEM operating at 200 kV. The heat dissipation measurement was done at room temperature (24 °C) using our lab-made instrument where applied current was 7 A, turn in coil was 140 and the frequency of AC field was 50 Hz. The maximum field can be generated by this instrument is about 92 kA/m.

3. Experiment

3.1. Material synthesis method

We have used here diphenylether/EtOH/H_2O (18:1:1 in volume ratio) as solvent and total volume was made 20 ml. Expecting control over micellar-core sizes by varying CTAB concentration the FePt particles were synthesized at two different concentrations of CTAB (set A 10^{-1} M, B 10^{-2} M) keeping all other conditions fixed. The iron source $Fe(acetate)_2$ (0.5 mmol) and platinum source $Pt(acac)_2$ (0.5 mmol) were introduced in reactor to obtain Fe and Pt in the particles of equal proportion by reducing the corresponding salts. The reaction was performed under N_2 atmosphere with heating the reaction mixture under stirring condition. The reducing agent sodium borohydride (1.5 mmol) solution in water was added drop by drop after the temperature of reaction mixture reached to 100 °C. After addition of reducing agent the reaction mixture turned to black indicating formation of FePt nanoparticles. This mixture was refluxed at 240 °C for 4 hr. At the end 2 ml of oleic acid was added to functionalize the particles to make them biocompatible. The particles were precipitated by adding EtOH and separated out by centrifugation and dispersed in hexane and again centrifuged to remove the excess unbound water insoluble organic part. The particles were purified by rewashing with EtOH and hexane alternatively. The resulting dried particles were subjected to heat treatment at 550 °C for 30 min under N_2 atmosphere. Those as made and annealed particles were subjected for different measurement like EDAX, XRD and magnetic. For TEM measurement much diluted ethanol dispersion of particles was dropped on C-coated copper grid and dried in vacuum.

3.2. Cell culture and cell imaging experiment

The human mammary carcinoma cells (MDAMB-231) were obtained from National Centre for Cell Science (NCCS, Pune, India) and was maintained in Dulbecco's Modified Eagle's Medium (DMEM) containing 100 ml/L of fetal bovine serum (FBS) in a humidified atmosphere of 5% CO_2 in cell culture incubator. Cell imaging was investigated by treating the human mammary carcinoma cells (MDAMB-231) with sodium oleate functionalized and RITC tagged 10 nm FePt fct phase particles incubating the cell for 24 h.

4. Result and discussion

The solution phase metal salts reduction and carbonyl precursor decomposition are well known technique to synthesize FePt magnetic alloyed particles [19–23]. But carbonyl precursors are highly toxic and due to its high volatility it is difficult to maintain the composition of metals in final products using the carbonyl precursors. We have used Fe $(acetate)_2$ as Fe source and $Pt(acac)_2$ as Pt source and the reducing agent sodium borohydride to synthesize FePt particles. Here the reducing agent completely reduces both Fe and Pt precursor salts at higher temperature. We performed the reaction using same method but at low temperature (~80 °C) where the result was not consistent. We measured the Fe and Pt composition at final product by EDX method. The particles produced at low temperature were highly Pt rich and sizes of particles were not also uniform. EDX measurement performed on the samples prepared in 240 °C shows far better and consistent results with little error. Different regions of particles deposited on copper grid were investigated and average value was tabulated. The data is shown in Table 1. It shows composition of Fe:Pt is on an average about 50:50. The particle sizes were investigated by TEM analysis. TEM images are shown in Fig. 1 (a, b). The histogram was done for both the sets taking in count of about 50 particles from each of sets. The average particle sizes for two different concentrations of micelles for sets A and B are 4 ± 0.5 and 8 ± 0.7 nm respectively. Here it is observed that as the concentration of surfactants decreases the particle size increases. It is well known that solution of water containing reversed micelles is employed as suitable reaction media for the synthesis of size controlled nanoparticles [24]. The control in particle size is achieved by creating micellar core of two different sizes and carrying the reaction inside the core. As a consequence of micellar dynamic motion the reactant can come in contact and react to each other forming the nuclei of nanoparticles. By the same dynamic process these precursor nuclei are accumulated in some closed micellar core leading to the formation of stable nanoparticles of limited growth. This is the way how micelles provide control over particle size. Empirically it has been found that the

Table 1
Atomic composition for two different samples from EDAX measurement in SEM.

Elements	Atomic % for sample 4 nm	Atomic % for sample 8 nm
Fe	47.77	51.8
Pt	52.22	48.2

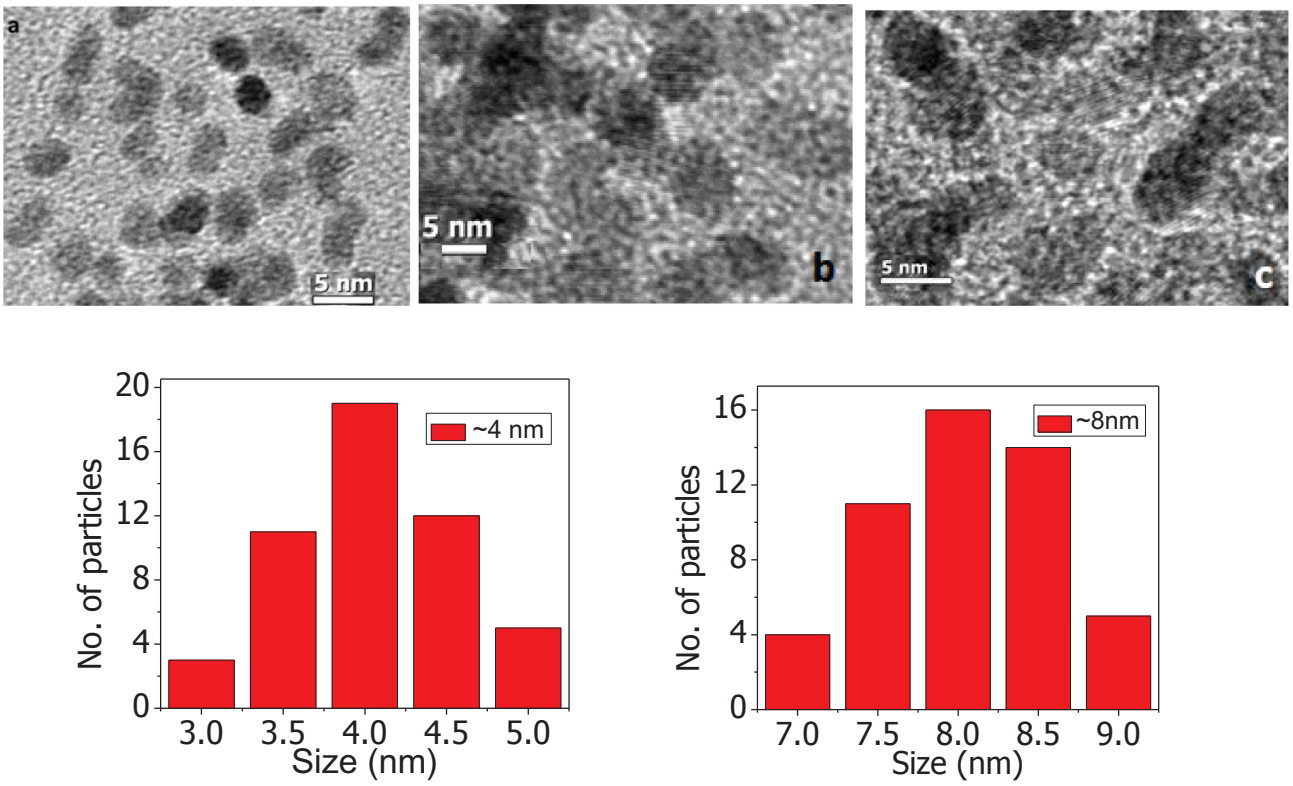

Fig. 1. TEM images for 2 sets of nonannealed samples of 4 nm (a), 8 nm (b) and for one set of annealed sample of 4 nm (c) and histogram for 4 nm and 8 nm particles.

most relevant external parameters allowing size modulation are concentration of surfactant in solution which controls the micellar core size, number of micelles formation, concentration of reactant, collision of reactants etc. though the micro structure of mixture containing surfactant, oil and water has been the subject of many debates [25]. One of the representative images after annealing the 4 nm particles are shown in Fig. 1c, which indicates particle size of about 5 nm ± 0.7 with very little increase in size compare to the non-annealed particles. This increase in size occurs due to tetragonal expansion but no significant agglomeration takes place after annealing the sample.

XRD measurement was done scanning from 2θ = 20 to 60° before and after annealing the sample. The particle size was calculated considering [1 1 1] peak from XRD by using Debye Scherer formula. The size obtained from XRD data tally well with the size measured from TEM. One of the representative XRD pattern for both the annealed and non-annealed samples is shown in Fig. 2(a, b). The peaks are indexed comparing with JCPDS data which reveals that for nonannealed sample, two peaks at 2θ = 40 and at 47° indicating (1 1 1) and (2 0 0) planes and for annealed samples all the peaks corresponding to the planes (0 0 1), (1 1 0), (1 1 1), (2 0 0) (0 0 2) are evolved. This indicates that the as made non-annealed particles has a disordered face centered cubic (fcc) crystal structure whereas annealed sample has ordered face centered tetragonal (fct) or $L1_0$ phase. In fcc phase the atoms of Fe and Pt in crystal are randomly oriented where as in fct phase they are ordered and tetragonally elongated along z axis. Tetragonal crystal lattices result from stretching a cubic lattice along one of its lattice vectors, so that the cube becomes a rectangular with a square base (*a* by *a*) and height (*c*, which is different from *a*). XRD measurement for the 8 nm particles after annealing the sample is shown in Fig. 2(c) to compare the order parameter with increase of particle size. Here we see for higher size particles the order parameter is higher which is indicated by increase of integrated peak area for both the 111 and 200 peaks.

The magnetic hysteresis loop measurements (Fig. 3) for non-annealed and annealed samples shows the increase in coercivity to very high magnitude after annealing the samples. The coercivity becomes almost 2.5 kOe and 5 kOe for the 4 and 8 nm of annealed samples respectively. The increase in high coercivity supports ordering of particles from fcc crystal structure to $L1_0$ phase. The $L1_0$ structure is tetragonally elongated along z axis, which produce very high magnetic crystalline anisotropy and hence such high value of coercivity. More over as the particles are very small and single domain in nature, magnetization takes place only by rotations of unit magnet. AC magnetic field dependent measurement is also an important criterion for the use of particles in hyperthermia therapy. It is known that magnetic materials display a magnetic hysteresis when subjected to an AC magnetic field. The area enclosed in this hysteresis loop represents the irreversible work, which is dissipated in the environment as thermal energy which profitably can be used in magnetic hyperthermia. This loss power (LP) is related to the "Specific Absorption Rate" (*SAR*) and SAR can be calculated with the equation, SAR = S. ΔT/Δt where S is specific heat capacity and ΔT is change in temperature in time t. The LP can be calculated from the equation LP = *Af*, where *A* is the area of the hysteresis loop and *f* the frequency of the magnetic field [26,27]. Here we see for 8 nm fct phase particles, high hysteresis loop area is produced compared to the 4 nm fct phase particles. As we are interested to use the particles for hyperthermia therapy we have done some measurements on heat dissipation by the particles under AC magnetic field in our lab made set-up where we can produce nearly 90 kA/m AC magnetic field at nearly 50 Hz of AC field frequency. For this measurement 1 mg of each sample was taken in 2.5 ml of water in dispersed condition to have an idea about dissipation of heat by the particles under AC magnetic field. The heat dissipations curves are shown in Fig. 4. From this measurement we see that the heat dissipation rate for fct phase particles is much more higher compared to fcc phase. The heat dissipation rate for fcc phase is not significant but for fct phase, the amounts are reasonably significant for both the sizes 8 nm and 4 nm. From these two heat dissipation curves for 8 nm and 4 nm fct phase particles, we have calculated SAR from the equation SAR = S.ΔT/Δt, where S is specific heat capacity of water since temperature raised was measured in water sample taking 1 mg of each sample in dispersed condition, ΔT is the

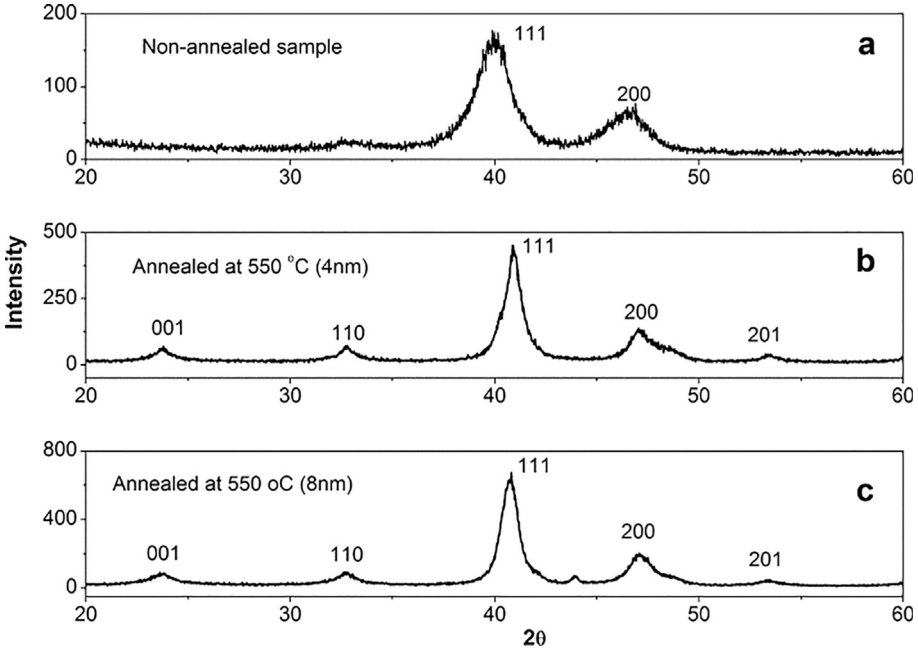

Fig. 2. XRD curves for nonannealed 4 nm (a), annealed 4 nm (b), and annealed 8 nm (c), particles prepared at two different concentrations of CTAM surfactant.

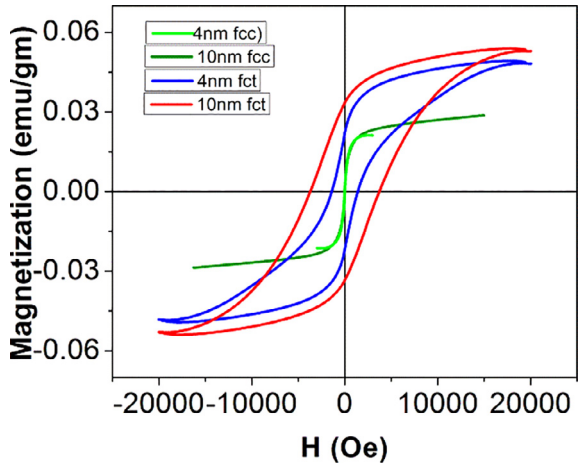

Fig. 3. M-H loop for two sets of particles before annealing and after annealing the samples (4 nm and 8 nm both).

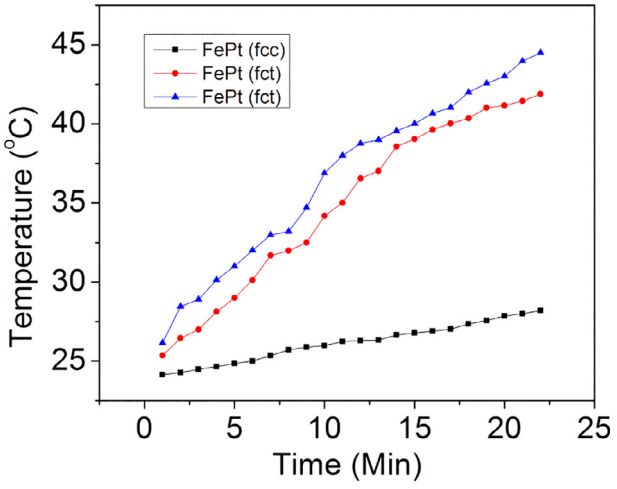

Fig. 4. Heat dissipation data for 4 nm nonannealed fcc sample, 4 nm annealed fct and 8 nm annealed fct samples.

change in temperature in time Δt. The SAR values were found to be 153 W/g for 8 nm particle and 137 W/g for 4 nm particles. The loss power (LP) was calculated from the equation A.f where A is hysteresis loop area and f is frequency from Fig. 3. The calculated values were 4.3 W/g and 2.6 W/g for 8 and 4 nm fct phase particles for maximum applied field 20 kOe which is much lower compared to 90 kA/m. Since hysteresis loop measurement and heat dissipation measurements were done from two different instruments so it is not possible to compare the values. But here it is observed that for 8 nm particles both SAR and LP values are higher compared to those for 4 nm particles. Hence from these data we can predict that higher the loss power the higher is the value of SAR. From these data we can predict that heating rate can be controlled by tuning the magnetic properties and can be used for hyperthermia therapy by tuning their magnetic properties with change of particle size and structure. Higher the heating rate higher will be the killing rate of cancer cells. Hence injecting these particles directly to the carcinoma tumor the cancer cells can be destroyed with faster rate applying AC magnetic field from outside the body.

Aiming the use of particles for hyperthermia therapy, we need to check the internalization of the particles with the cells for better heat dissipation from particles to cells. To check that we have made the particles water soluble by functionalizing the particles with oleic acid followed by addition of sodium bicarbonate. As particles are functionalized with oleic acid they form the sodium oleate after addition of sodium bicarbonate and become water soluble then the particles are tagged with RITC dye and incubated with cancer cell line to check the internatiozation of particles with cell. The fluorescence image of the cancer cell line after incubating them with this RITC tagged particles are shown in Fig. 5 which reveals that very good internalization of the particles with cells. Hence these particles will be useful for hyperthermia therapy but before that clinical use more investigations are required but this result is very promising for use of these particles in hyperthermia therapy in future.

5. Conclusion

In this method we have been able to vary the particles sizes by varying the concentration of surfactant. The particles showed approximately 50:50 (Fe:Pt) composition and have a disordered fcc crystal structure. The fcc phase particles are superparamagnetic in nature.

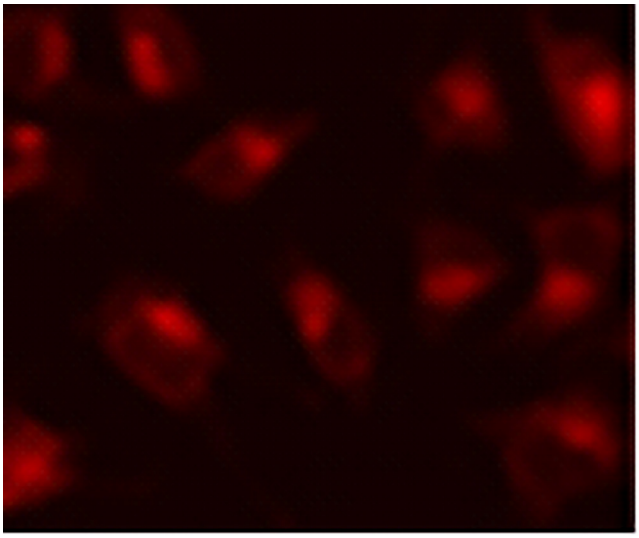

Fig. 5. Cell imaging by RITC tagged 4 nm nonannealed FePt particles.

Those particles upon annealing transfer to a chemically ordered $L1_0$ or fct phase with tetragonal crystal structure and showed an enormous increase in coercivity. Order parameter increases with increase of particles size. Hence we can prepare the particles of wide range of magnetic properties from superparamagnetic to highly hard ferromagnetic. We have characterized these particles from different directions aiming to use them in hyperthermia therapy. The AC magnetic field applied heating ability of the particles indicates their promising use for hyperthermia therapy and internalization of these functionalized particles with cancer cells opens up a new avenue in hyperthermic cancer treatment in a better way.

Acknowledgements

Authors are thankful to the Department of Science and Technology, India (DST), Government of India for the funding under the project SR/WOS-A/CS-158/2016 and S.N. Bose National Centre for Basic Sciences, Kolkata, India for the Project numbered SNB/MM/15-16/164-1.

Appendix A. Supplementary data

Supplementary data to this article can be found online at https://doi.org/10.1016/j.jmmm.2018.11.024.

References

[1] (a) N. Guan, Y. Wang, D. Sun, J. Xu, Nanotechnology 20 (2009) 105603;
(b) S. Xuan, Y.X.J. Wang, J.C. Yu, K.C.F. Leung, Langmuir 25 (2009) 11835.
[2] E. Katz, I. Willner, Angew. Chem. Int. Ed. 43 (2004) 6042–6108.
[3] (a) S. Mornet, S. Vasseur, F. Grasset, E. Duguet, J. Mater. Chem. 14 (2004) 2161–2175;
(b) Q. Pankhurst, J. Connolly, S. Jones, J. Dobson, J. Phys. D: Appl. Phys. 36 (2003) R167–R181.
[4] (a) C. Xu, K. Xu, H. Gu, X. Zhong, Z. Guo, R. Zheng, X. Zhang, B. Xu, J. Am. Chem. Soc. 126 (2004) 3392–3393;
(b) S. Bucak, D. Jones, P. Laibinis, T. Hatton, Biotechnol. Prog. 19 (2003) 477–484.
[5] (a) J. Perez, L. Josephson, R. Weissleder, Chem. Biol. Chem. 5 (2004) 261–264;
(b) J. Perez, T. O'Loughin, F. Simeone, R. Weissleder, L. Josephson, J. Am. Chem. Soc. 124 (2002) 2856–2857.
[6] (a) R. Rosensweig, J. Magn. Magn. Mater. 252 (2002) 370–374;
(b) N. Nitin, L. LaConte, O. Zurkiya, X. Hu, G. Bao, J. Biol. Inorg. Chem. 9 (2004) 706–712.
[7] W.J.M. Mulder, G.J. Strijkers, G.A.F. Van Tilborg, D.P. Cormode, Z.A. Fayad, K. Nicolay, Acc. Chem. Res. 42 (2009) 904–914.
[8] R.A. Sperling, P. Riveragil, F. Zhang, M. Zanella, W. Parak, J. Chem. Soc. Rev. 37 (2008) 1896–1908.
[9] J.H. Gao, H.W. Gu, B. Xu, Acc. Chem. Res. 42 (2009) 1097–1107.
[10] J. Kim, Y. Piao, T. Hyeon, Chem. Soc. Rev. 38 (2009) 372–390.
[11] R. Weissleder, U. Mahmood, Radiology 219 (2001) 316–333.
[12] J. Cheon, J.H. Lee, Acc. Chem. Res. 41 (2008) 1630–1640.
[13] S. Sun, Science 287 (2000) 1989.
[14] M. Chen, D.E. Nikles, Nano Lett. 2 (2002) 211.
[15] M. Mandal, S. Kundu, S.K. Ghosh, K. Esumi, T. Pal, Langmuir 18 (2002) 7792.
[16] M. Mandal, S. Kundu, T.K. Sau, S.M. Yusuf, T. Pal, Chem. Mater. 15 (2003) 3710.
[17] M. Mandal, S. Kundu, S.K. Ghosh, T.K. Sau, S.M. Yusuf, T. Pal, J. Coll. Int. Sc. 286 (2005) 187.
[18] (a) M.P. Pileni, Langmuir 17 (2001) 7476. (b) M.P. Pileni, (Ed.), Elsevier, New York, 1989.
[19] C. Petit, P. Lixon, M.P. Pileni, Langmuir 7 (1991) 2620.
[20] S. Sun, S. Anders, T. Thomson, J.E.E. Baglin, M.F. Toney, H.F. Hmann, C.B. Murray, B.D. Terris, J. Phys. Chem. B 107 (2003) 5419.
[21] B. Jeyadevan, A. Hobo, K. Urakawa, C.N. Chinnasamy, K. Shinoda, K.J. Tohji, Appl. Phys. 93 (2003) 7574.
[22] T. Iwaki, Y. Kakihara, T. Toda, M. Abdullah, K. Okuyama, J. Appl. Phys. 94 (2003) 6807.
[23] K.E. Elkins, T.S. Vedantam, J.P. Liu, J. Zeng, S. Sun, Y. Ding, Z.L. Wang, Nano Lett. 3 (2003) 1647.
[24] M. Nakaya, Y. Tsuchiya, K. Ito, Y. Oumi, T. Sano, T. Teranishi, Chem. Lett. 33 (2004) 130.
[25] (a) M. Nakaya, T. Teranishi, Trans. Mater. Res. Soc. Jpn. 30 (2005) 579;
(b) F. Ferrate, V.T. Liveri, Colloid Surf. A 259 (2005) 7.
[26] R. Hergt, S. Dutz, R. Müller, M. Zeisberger, J. Phys.: Condens. Matter 18 (2006) S2919–S2934.
[27] L. Alon, D.K. Sodickson, C.M. Deniz, Bioelectromagnetics 37 (2016) 493–503.